Molecular Immunology 113 (2019) 22–30

Contents lists available at ScienceDirect

Molecular Immunology

journal homepage: www.elsevier.com/locate/molimm

The 20S immunoproteasome and constitutive proteasome bind with the same affinity to PA28αβ and equally degrade FAT10

Gunter Schmidtke[a], Richard Schregle[a], Gerardo Alvarez[a], Eva M. Huber[b], Marcus Groettrup[a,c,*]

[a] Division of Immunology, Department of Biology, University of Konstanz, D-78457, Konstanz, Germany
[b] Center for Integrated Protein Science Munich at the TUM Department of Chemistry, Technical University of Munich, D-85748, Garching, Germany
[c] Biotechnology Institute Thurgau at the University of Konstanz (BITg), CH-8280, Kreuzlingen, Switzerland

ARTICLE INFO

Keywords:
20S proteasome
Immunoproteasome
LMP2
LMP7
PA28αβ
FAT10

ABSTRACT

The 20S immunoproteasome (IP) is an interferon(IFN)-γ − and tumor necrosis factor (TNF) −inducible variant of the 20S constitutive proteasome (CP) in which all its peptidolytically active subunits β1, β2, and β5 are replaced by their cytokine inducible homologues β1i (LMP2), β2i (MECL-1), and β5i (LMP7). These subunit replacements alter the cleavage specificity of the proteasome and the spectrum of proteasome-generated peptide ligands of MHC class I molecules. In addition to antigen processing, the IP has recently been shown to serve unique functions in the generation of pro-inflammatory T helper cell subtypes and cytokines as well as in the pathogenesis of autoimmune diseases, but the mechanistic involvement of the IP in these processes has remained elusive. In this study we investigated whether the IP differs from the CP in the interaction with two IFN-γ/TNF inducible factors: the 11S proteasome regulator PA28αβ and the ubiquitin-like modifier FAT10 (ubiquitin D). Using thermophoresis, we determined the affinity of PA28αβ for the CP and IP to be 12.2 nM +/− 2.8 nM and 15.3 nM +/− 2.7 nM, respectively, which is virtually identical. Also the activation of the peptidolytic activities of the IP and CP by PA28αβ did not differ. For FAT10 we determined the degradation kinetics in cycloheximide chase experiments in cells expressing almost exclusively IP or CP as well as in IFN-γ stimulated and unstimulated cells and found no differences between the degradation rates. Taken together, we conclude that neither differences in the binding strength to, nor activation by PA28αβ, nor a difference in the rate of FAT10-mediated degradation can account for distinct functional capabilities of the IP as compared to the CP.

1. Introduction

Pro-inflammatory cytokines like IFN-γ and TNF have a major impact on protein degradation and fragmentation in the context of an immune response. They lead to a coordinated up-regulation of numerous factors involved in antigen presentation on MHC class I molecules including the ubiquitin-like modifier FAT10 (also called ubiquitin D (UBD)), the three proteolytically active subunits of the immunoproteasome (IP), the two subunits of the 11S proteasome regulator PA28αβ, the cytosolic leucine aminopeptidase, and the ER aminopeptidases ERAP1 and ERAP2. A pertinent question posed by this joint induction is whether there is a preferential functional cooperation between these factors. Centrally involved in generating peptide ligands of MHC class I molecules is the 26S proteasome (Collins and Goldberg, 2017). It consists of a barrel-shaped core protease, the 20S proteasome, and one or two copies of the 19S regulator which bears receptors for poly-ubiquitin chains and FAT10, ubiquitin deconjugating enzymes, and a ring of ATPases involved in substrate unfolding (Schweitzer et al., 2016). Most tissues express predominantly the constitutive 20S proteasome (CP) with its three proteolytically active subunits β1, β2, and β5 bearing the proteasomal caspase-like, trypsin-like, and chymotrypsin-like activities, respectively (Kremer et al., 2010; Stohwasser et al., 1997). Upon infection of mice with viruses, bacteria or fungi, the CP is largely replaced in infected tissues by the IP featuring the peptidolytic subunits β1i (LMP2), β2i (MECL-1), and β5i (LMP7) (Khan et al., 2001) (Barton et al., 2002). These subunit exchanges lead to an enhancement of the proteasomal chymotrypsin-like and trypsin-like activities and a suppression of the caspase-like activity (Driscoll et al., 1993; Gaczynska et al., 1993; Groettrup et al., 1995), which enables the generation of more MHC class I ligands required for enhanced class I cell surface expression in IFN-γ and TNF stimulated tissues (Boes et al., 1994; Fehling et al., 1994; Tenzer et al., 2004; Toes et al., 2001). Apart from the marked effect of the IP on antigen processing, which can be pivotal for the presentation of certain antigenic peptides (Groettrup et al., 2010), additional functions of the IP have recently been discovered. IPs were found to be required for the normal production of the pro-

* Corresponding author at: Division of Immunology, Department of Biology, University of Konstanz, Universitaetsstrasse 10, D−78457 Konstanz, Germany.
E-mail address: Marcus.Groettrup@uni-konstanz.de (M. Groettrup).

https://doi.org/10.1016/j.molimm.2017.11.030
Received 31 August 2017; Received in revised form 27 November 2017; Accepted 28 November 2017
Available online 06 December 2017

inflammatory cytokines TNF, IFN-γ, IL-6, IL-17, and IL-23 (Koerner et al., 2017; Muchamuel et al., 2009), for the differentiation of the pro-inflammatory T helper cell lineages Th1 and Th17 (Kalim et al., 2012; Vachharajani et al., 2017), and for the pathogenesis of several autoimmune diseases in pre-clinical models like diabetes, rheumatoid arthritis (Muchamuel et al., 2009), inflammatory bowel disease (Basler et al., 2010; Fitzpatrick et al., 2006; Schmidt et al., 2010), multiple sclerosis (Basler et al., 2014), systemic lupus erythematosus (Ichikawa et al., 2012), and Hashimoto's thyroidits (Nagayama et al., 2012). It is enigmatic, how the IP is mechanistically involved in these processes, but one possibility would be a selective binding or functional cooperation with other, potentially cytokine-inducible factors, which may lead to an IP-selective partial processing or degradation of substrates.

One candidate for such a factor would be the 11S proteasome regulator (Dubiel et al., 1992), also designated PA28αβ (Ma et al., 1992). PA28αβ is a heptameric circular proteasome regulator which is assembled from the two non-ATPase subunits PA28α and PA28β (Ahn et al., 1996; Kuehn and Dahlmann, 1996; Song et al., 1996; Zhang et al., 1999). The recently determined crystal structure of PA28αβ revealed an alternating arrangement of four α and three β chains (Huber and Groll, 2017). PA28 subunits bind to the outer α-rings of the barrel-shaped 20S proteasome by inserting their C-termini into pockets formed by the α-subunits of the proteasome. Activation loops of PA28αβ then trigger the opening of the otherwise closed 20S proteasome which allows trafficking of polypeptides through the 2 nm wide pore of the PA28αβ ring into the lumen of the IP or CP (Gray et al., 1994; Knowlton et al., 1997; Sprangers and Kay, 2007; Whitby et al., 2000). This is probably the reason why PA28αβ activates the hydrolysis of fluorogenic peptides by the 20S proteasome traditionally used to measure its caspase-like, trypsin-like, and chymotrypsin-like activities to a similar extent (Realini et al., 1997). PA28αβ affects the peptide generation by the 20S proteasome *in vitro* (Cascio et al., 2002; Dick et al., 1996; Groettrup et al., 1995) and is required for efficient presentation of T cell epitopes from a number of viral, bacterial, and tumor-derived antigens (de Graaf et al., 2011; Groettrup et al., 1996b; Murata et al., 2001; Schwarz et al., 2000; van Hall et al., 2000; Yamano et al., 2002). While for PA28γ, a homoheptameric homologue of PA28αβ, several protein degradation substrates have been reported (Li et al., 2006; Moriishi et al., 2003; Zhang and Zhang, 2008), no stably folded proteins are known to date which are targeted for proteasomal degradation via PA28αβ. However, since it is quite possible that also PA28αβ mediates specific protein degradation, it is important to investigate if PA28αβ preferentially binds to the CP or IP. Using recombinant PA28αβ to activate purified mouse IP and CP in vitro, Stohwasser et al. found identical activation kinetics for the IP and CP suggesting equal binding affinities (Stohwasser et al., 2000). Yet, Fabre et al. reported recently that after formaldehyde-mediated protein cross-linking in intact cell lines expressing equal amounts of IP and CP, PA28αβ was bound to IP at a fourfold greater amount than to CP when analyzed by gradient centrifugation or co-precipitation (Fabre et al., 2015). This result warrants a direct measurement of the affinity of PA28αβ to the IP and CP which to our knowledge has not been accomplished yet.

A second factor investigated in this study for functional cooperation with the IP as compared to the CP is the ubiquitin-like modifier FAT10. FAT10 consists of two ubiquitin-like domains joined by a short linker (Groettrup et al., 2008; Theng et al., 2014). It gets isopeptide-linked to lysines of hundreds of substrate proteins via its free C-terminal GG motif with the help of the E1 activating enzyme UBA6 and the E2 conjugating enzyme USE1 (Aichem et al., 2012; Aichem et al., 2010; Chiu et al., 2007). FAT10 is the only ubiquitin-like modifier known to date which directly targets its conjugation substrates for degradation by the 26S proteasome without the need for ubiquitylation (Hipp et al., 2005; Rani et al., 2012). In contrast to the fairly long-lived ubiquitin, which gets cleaved from its degradation substrates at the proteasome and is recycled, monomeric FAT10 is degraded at the same rate as FAT10-conjugates with a half-life of one hour (Aichem et al., 2014; Schmidtke et al., 2009). No evidence for deconjugation of FAT10 at the 26S proteasome could be obtained suggesting that it is degraded by the proteasome along with its substrates. The fusion of FAT10 with two different long-lived viral proteins led to their accelerated degradation by the proteasome and to markedly enhanced presentation of peptides from these antigens on MHC class I molecules suggesting that FAT10-mediated degradation feeds into the class I presentation pathway (Ebstein et al., 2012; Schliehe et al., 2012). FAT10 is strongly and synergistically induced with IFN-γ and TNF in many tissues (Liu et al., 1999; Raasi et al., 1999) and is also up-regulated upon the maturation of dendritic cells and medullary thymic epithelial cells (Bates et al., 1997; Lukasiak et al., 2008). Consistently, FAT10 deficiency affects the selection of immature thymocytes in a T cell receptor specificity-dependent manner (Buerger et al., 2015). Whether FAT10 is preferentially degraded by the 26S IP or CP has not yet been investigated. In this study we show that FAT10 is degraded at the same pace in cells expressing almost exclusively IP or CP. Moreover, we show that IP and CP bind to PA28αβ with the same affinity and are equally activated by this 11S proteasome regulator.

2. Material and methods

2.1. Mice, cell lines and cytokines

C57BL/6 mice (H-2^b) were originally purchased from Charles River. *Lmp7* (Fehling et al., 1994), and *Mecl-1* (Basler et al., 2006) gene-targeted mice were provided by J. Monaco (Cincinnati, OH, USA). *Lmp7*$^{-/-}$/*Mecl-1*$^{-/-}$ double deficient mice (L7 M$^{-/-}$) were generated by crossing the F1 generation of *Lmp7*$^{-/-}$ x *Mecl-1*$^{-/-}$ mice. For induction of the IP in the liver, BALB/c mice were i.v. infected with 200 pfu lymphocytic choriomeningitis virus (LCMV)-WE eight days before sacrifice. Mice were kept in a specific pathogen-free facility and used at 8–12 weeks of age. Animal experiments were approved by the review board of Regierungspräsidium Freiburg. LCL721.145 and LCL721.174 are subclones of the human B-lymphoblastoid cell line LCL721 (Kavathas et al., 1980). The human embryonic kidney cell line HEK293T was originally purchased from ATCC. Cells were cultured in Iscove's Modified Dulbecco's Medium (IMDM) with GlutaMAX supplemented with 10% FCS and 100 U/ml penicillin/streptomycin. Media and supplements were purchased from Invitrogen-Life Technologies. Recombinant mouse IFN-γ was purchased from Peprotech and used at 400 U/ml.

2.2. Cloning, expression, and purification of PA28αβ

For co-expression of mouse PA28 α and β subunits, the respective genes *Psme1* and *Psme2* were inserted into the pETDuet-1 vector (Novagen) as previously described (Huber and Groll, 2017). Validated plasmids were transformed into *E. coli* BL21 (DE3) and single clones were grown in liquid LB medium at 37 °C to an optical density (600 nm) of about 0.5–0.7. Gene expression was induced for 4 h at 37 °C by 1 mM IPTG. Finally, cells were harvested and frozen at −20 °C until further use.

PA28αβ complexes were purified as previously described (Huber and Groll, 2017). Briefly, cells were resuspended in 20 mM Tris(hydroxymethyl)-aminomethane (Tris)/HCl pH 7.5 supplemented with 1 mM dithiothreitol (DTT) and lysed by sonification. Upon centrifugation (20 min at 21,000g; 4 °C), the cell lysate was loaded onto a 20 ml Q-Sepharose column (GE Healthcare). Bound proteins were eluted by increasing the salt concentration to 500 mM in 7.5 column volumes (CVs). Fractions containing PA28 subunits were dialysed against 5 mM KH_2PO_4/K_2HPO_4 pH 7.5, 50 mM NaCl and 1 mM DTT and loaded onto a 20 ml hydroxyapatite column (BioRad). By applying a linear gradient over 7.5 CV to 300 mM KH_2PO_4/K_2HPO_4 pH 7.5 50 mM NaCl and 1 mM DTT, bound proteins were eluted. PA28αβ samples were concentrated by 10 kDa centrifugal filter devices and subjected to size exclusion

chromatography (Superdex 200 16/60; GE Healthcare) with 20 mM Tris/HCl pH 7.5, 100 mM NaCl and 1 mM DTT. Except for gel filtration, all purification steps were carried out at 4 °C. Optionally, final polishing was achieved by Resource Q (1 ml; GE Healthcare) chromatography using a gradient from 0 to 1 M NaCl in 20 mM Tris/HCl pH 7.5 and 1 mM DTT over 60 CVs. For long-term storage, PA28αβ samples were supplemented with 20% glycerol and flash-frozen in liquid nitrogen.

2.3. Proteasome purification, activity assays, and affinity measurement

Mouse CP and IP were purified from livers of naïve *Lmp7*$^{-/-}$/*Mecl-1*$^{-/-}$ or BALB/c mice which had been infected eight days before sacrifice with 200 pfu LCMV-WE, respectively, exactly as previously described (Schmidtke et al., 2000). The purity and subunit composition of the CP and IP samples were analyzed on Coomassie-stained two-dimensional NEPHGE/SDS-PAGE and were very similar to the preparations that have been used previously for structural analyses (Huber et al., 2012).

The measurement of the catalytic activities of fluorophore-labelled and unlabelled IP and CP was performed as described before (Schmidtke et al., 2000), except that the digests were performed in MST-buffer (50 mM Tris/HCl pH 7.4, 150 mM NaCl, 10 mM $MgCl_2$, 0.05% Tween 20) which is the same buffer as used for the thermophoresis experiments (see below). A mixture (20 µl) of constant amounts of 20S proteasome and titrated amounts of mouse recombinant PA28αβ were incubated for one hour in the dark in a 384 well plate. After one hour, 20 µl of either 200 µM Succinyl-Leu-Leu-Val-Tyr-7-amino-4-methylcoumarin (Suc-LLVY-AMC) or 20 µl of 200 µM Z-Val-Gly-Arg-AMC (Z-VGR-AMC) was added to measure the chymotrypsin- or trypsin-like activity of the proteasome, respectively. The activity was determined as the increase in fluorescence due to the release of the AMC fluorogenic leaving group. The fluorescence was determined with a TECAN Infinite® M 200 PRO plate reader at 30, 60, and 90 min after initiation of the reaction by adding the substrate, using emission and excitation wavelengths of 360 nm and 465 nm, respectively, for AMC. The reaction was incubated at 37 °C. Values from the linear range of the reaction were used to calculate the activities. Triplicates were measured for all data points.

For thermophoresis experiments, the proteasome was labelled as described in the manual of the Monolith protein labelling kit blue-NHS (Nanotemper Technologies). The proteasome was concentrated to 1 mg/ml using Amicon ultra centrifugal filters (Amicon). The filters had an exclusion limit of 30 kDa. The buffer was exchanged to the labelling buffer supplied in the kit. We used 100 µl of 1 mg/ml of proteasome and a fivefold molar excess of the labelling dye. The labelling was performed for 1 h at room temperature in the dark. Then, the buffer was exchanged to the MST-buffer (see above) supplemented with 20% glycerol, as recommended by the supplier of the Monolith Nt. 115 instrument (Nanotemper Technologies, Munich). The concentration of IP and CP was adjusted to 500 µg/ml. The proteasome and PA28αβ, both in MST-buffer with 20% glycerol, were stored at −80 °C. The protein concentration was determined with the Pierce BCA protein assay kit (Thermo Scientific). For the binding assay, a serial twofold dilution of the not labelled binding partner, PA28αβ, in MST-buffer/20% glycerol was prepared and 10 µl aliquots of each dilution series were dispensed into 15 small micro reaction tubes. The undiluted PA28αβ had a concentration of 2.5 µM (0.5 µg/µl). The 20S proteasome (0.5 µg/ml) was diluted 1:100 in MST-buffer/20% glycerol yielding a concentration of 7.14 nM, and 10 µl of diluted proteasome was mixed with each dilution of PA28αβ. The binding was allowed to proceed for one hour at RT in the dark. We used the Monolith Nt. 115 instrument for the measurement of the titration curve. The setting on the Monolith instrument was 80% power for the detection laser, yielding a signal of about 320 fluorescence units for the fluorophore-labelled proteasome at the used dilution. The MST-laser power was set to 20% or 40% for the analysis of the binding curve. The samples of the PA28αβ dilution series mixed with labelled proteasomes were centrifuged at 20 000 ×g in an Eppendorf 5417R centrifuge for 15 min, and filled into capillaries by aspiration. The affinity constants were calculated using the software provided by Nanotemper Technologies. Both experiments, the thermophoresis and the measurement of the proteolytic activities were performed with two different preparations of PA28αβ, and two different preparations of IP and CP.

2.4. Cloning of lentiviral vector construct and production of lentiviral particles

The coding sequence of human FAT10 with a C-terminal 6xHis-3xFlag tag was cloned from pcDNA3.1-6xHis-3xFlag-FAT10 (Chiu et al., 2007) into the *NheI* and *NotI* sites of the HIV-based lentiviral expression vector pCDH-EF1α-MCS-IRES-copGFP (System Biosciences) to get pCDH-EF1α-hFAT10-IRES-cGFP. The vector sequence was verified by sequencing (GATC Biotech).

Lentiviral particles were produced by transient co-transfection of the expression vector pCDH-EF1α-hFAT10-IRES-cGFP, the envelope vector pMD2.G, and the packaging vector psPAX2 into HEK293T cells using polyethylenimine (PEI; linear, MW 25,000, Polysciences). For this purpose HEK293T cells were cultured in Iscove's Modified Dulbecco's Medium (IMDM) containing GlutaMAX (Gibco – Life Technologies) supplemented with 10% FCS, 100 U/mL penicillin, and 100 mg/ml streptomycin and grown to 80–90% confluency. Prior to transfection the medium was changed to antibiotics-free IMDM supplemented with 10% FCS. For transfection, lentiviral vector DNA was mixed at a ratio of 1 µg pMD2.G: 1.84 µg psPAX2: 2.1 µg expression vector in serum-free IMDM, then mixed with PEI at a ratio of 3 µg PEI: 1 µg vector DNA, and dropwise added to the cells. After 8–16 h, the medium was removed and the cells replenished with IMDM supplemented with 15% FCS, 100 U/mL penicillin, and 100 mg/ml streptomycin. Supernatant containing lentiviral particles was harvested 48 h and 72 h post-transfection. In order to purify lentiviral particles, contaminating vector DNA was digested by adding 1 µg/ml DNase I (Roche) and 1 mM $MgCl_2$ for 20 min at 37 °C. Then, the supernatant was sterile filtered (0.45 µm, polyethersulfone membrane) and mixed with 8% polyethylene glycol 6000 (PEG; average molecular weight 6000 Da) and 0.3 M NaCl to precipitate lentiviral particles overnight at 4 °C. Precipitated lentiviral particles were pelleted by centrifugation (4600 g, 25 min, and 4 °C). The cleared supernatant was discarded, and the pellet was dried for 5 min. Then the pellet was covered with 100–200 µl of cold PBS and dissolved overnight at 4 °C. On the next day, the lentiviral particles were carefully re-suspended and aliquoted, then snap-frozen in liquid nitrogen and stored at -80 °C. Lentiviral stocks were titrated in HEK293T cells using tenfold serial dilutions and measuring GFP-expressing cells by flow cytometry. For calculating the titer, dilutions resulting in 1 − 25% GFP-positive cells were used.

2.5. Transfection, SDS-PAGE, and western blot

LCL721.174 and LCL721.145 cells were infected with the lentiviral particles encoding human 3xFLAG-hFAT10 (described in Section 2.4) with an M.O.I. of 30. After three days of cultivation, the cells were treated with 50 µg/ml cycloheximide and chased for the indicated time periods. HEK293T cells were stimulated for two days with 400 U/ml IFN-γ (Peprotech), transfected with the pcDNA3.1(+)-6xHis-3xFLAG-hFAT10 expression plasmid using the TransIT-LT1 transfection reagent (Mirus), and were then cultivated with IFN-γ for one more day. Subsequently, a cycloheximide chase experiment was performed. After harvest and washing with PBS, the cells were lysed in RIPA buffer (150 mM NaCl, 50 mM Tris pH 8, 1% (v/v) Nonidet P-40, 0.5% (v/v) sodiumdesoxycholate, 0.1% (w/v) SDS) including protease inhibitors (cOmplete EDTA-free, Roche). Lysates were centrifuged at 14,000 rpm for 15 min and supernatants were boiled with SDS sample buffer for 5 min at 95 °C. Proteins were separated by conventional reducing (1%

β-mercaptoethanol) SDS-PAGE and blotted onto nitrocellulose membranes (Whatman). After blocking in 1 × Roti-Block solution (Roth) for 1 h at RT, membranes were incubated with primary antibodies at 4 °C over night. Membranes were washed and probed with appropriate peroxidase-conjugated secondary antibodies for 2 h at RT. Membranes were washed again and proteins were visualized with enhanced chemiluminescence using SuperSignal West Femto solution (Thermo Scientific). Primary antibodies used were: anti-FLAG M2-HRP conjugate (Sigma) and anti-γ-tubulin (clone GTU-88, Sigma) followed by a second stage goat anti-mouse IgG-HRP conjugate (Dako).

3. Results

3.1. PA28αβ activates the CP and IP to the same extent and binds to them with the same affinity

The binding strength of PA28αβ to the 20S proteasome has only been determined via the cleavage of fluorogenic peptides, not via direct binding. This prompted us to use the relatively new method of thermophoresis to study the interaction of PA28αβ with the CP and IP. The method is based on the fact that the hydration shell of a molecule is changed as it binds to another molecule. This change leads to either faster or slower movement if the temperature of the solution is raised by a few centigrades. This movement is detected via a fluorophore in one of the binding partners. As a source of the IP, we purified the 20S proteasome from the liver of mice which had been infected with lymphocytic choriomeningitis virus (LCMV) eight days before sacrifice. Previously, we have shown that LCMV infection leads to an almost complete conversion of CP to IP in the liver (Khan et al., 2001). The CP was purified from the liver of LMP7$^{-/-}$MECL-1$^{-/-}$ doubly deficient mice, which are completely devoid of IP because in the absence of LMP7 and MECL-1 the precursor for LMP2 cannot be incorporated into the proteasome (De et al., 2003). The subunit compositions and purities of the mouse IP and CP were validated on two-dimensional non-equilibrium pH gradient gel electrophoresis (NEPHGE)/SDS-PAGE and were similar to previously documented preparations (Huber et al., 2012). The IP and CP preparations were labelled with the fluorophore Blue dye NT-495-NHS as described in the materials and methods section. To analyze whether the labelling changed the activity or the binding behaviour of the 20S proteasome, we performed proteolytic digests with fluorogenic peptides and increasing amounts of recombinant mouse PA28αβ purified from *E. coli* as described in the materials and methods section (Fig. 1). We compared the values obtained for labelled and unlabelled CP and IP, and found no difference, thus indicating that the covalently bound fluorophores did not affect the binding to and activation of 20S proteasomes. The specific activities for the CP, unlabelled or linked to the fluorophore, was 1.7 nM/hour/μg proteasome with Suc-LLVY-AMC as substrate, and 0.065 nM/hour/μg proteasome for Z-VGR-AMC. The respective values for the two types of IP were 0.35 nM/hour/μg proteasome and 0.025 nM/hour/μg proteasome. Therefore, the proteolytic activity of both CP and IP was not affected by the introduction of the fluorophore. Next, we analyzed the activation of all four types of proteasome by binding to titrated amounts of PA28αβ and found that the chymotrypsin-like (Fig. 1A) and trypsin-like (Fig. 1B) activities of mouse CP and IP were stimulated by PA28αβ similarly in a dose-dependent manner.

After we had shown that no difference between the unlabeled and fluorophore-linked proteasome preparations were apparent, we investigated the binding strength of mouse CP and IP to recombinant mouse PA28αβ via thermophoresis on a Nanotemper Monolith instrument. The binding curves for CP (Fig. 2A) and IP (Fig. 2B) were similar and the calculated affinity constants were 12.2 nM +/− 2.8 nM for CP and 15.3 nM +/−2.7 nM for IP which is virtually identical. In conclusion, CP and IP were equally strongly bound and activated by PA28αβ.

3.2. CP and IP degrade FAT10 at the same rate

Next, we compared the rates at which the IFN-γ/TNF inducible ubiquitin-like modifier FAT10 is degraded by CP and IP in two different human cell line systems. The first cell line system is based on the human B cell line LCL721, that originally had been obtained by *in vitro* infection of human peripheral blood lymphocytes with Epstein Barr Virus (Kavathas et al., 1980). The 20S proteasome of a sub-clone of this line, designated LCL721.145, was purified and its subunit composition was determined on Coomassie stained two-dimensional NEPHGE/SDS-PAGE. The migratory positions of 20S CP and IP subunits allow their assignment based on previous mass spectrometric analyses (Groettrup et al., 1996a) (Fig. 3A, right panel). Remarkably, LCL721.145 cells express barely detectable levels of the constitutive proteasome subunits β1 and β5 and very high levels of LMP2 and LMP7 indicating that they contain almost exclusively IP and hardly any CP. The subclone LCL721.174 has been obtained from parental LCL721 cells by γ-irradiation, which led to the loss of *Lmp2* and *Lmp7* genes (Kavathas et al., 1980). Accordingly, we could show with NEPHGE/SDS-PAGE that 20S proteasomes purified from LCL721.174 cells do not contain any LMP2 and LMP7. Since it has been shown that MECL-1 cannot be incorporated into the proteasome when LMP7 and LMP2 are missing (De et al., 2003; Groettrup et al., 1997), LCL721.174 contain exclusively CP and no IP. In order to express FAT10 in the CP-containing LCL721.174 and IP-containing LCL721.145 cells, we generated a lentiviral vector expressing human 3xFLAG-tagged FAT10 and GFP under the same promotor using an internal ribosome entry site (IRES) for GFP. Flow cytometric analysis of GFP expression confirmed a high transfection efficiency (data not shown). Three days after lentiviral infection, cycloheximide chase experiments were performed over a time period of four hours and FLAG-FAT10 expression was monitored on western blots (Fig. 3B). Consistent with previous radioactive pulse-chase and cycloheximide-chase experiments with tagged or endogenous FAT10, FLAG-FAT10 was degraded by the proteasome with a half-life of approximately one hour (Aichem et al., 2014; Hipp et al., 2005). The western blots and the densitometric evaluation of three independent experiments shown in Fig. 3B reveal that FLAG-FAT10 is degraded in the CP-containing LCL721.174 and IP-containing LCL721.145 cells at exactly the same rate indicating that CP and IP do not differ in their capability to degrade monomeric FAT10. In addition, the smear of FLAG-FAT10 conjugates was similarly degraded in both cell lines.

To investigate if cells, in which IP expression was induced by IFN-γ, would differ from uninduced cells with respect to the rate of FAT10 degradation, we performed experiments with the human embryonic cell line HEK293T. HEK293T cells express very low levels of IP and high levels of CP in the un-induced state, but over a three-day period of cultivation in the presence of IFN-γ, the CP is replaced largely by the IP as previously reported (Fabre et al., 2015) and confirmed by us (data not shown). HEK293T cells grown for three days in the presence or absence of IFN-γ were transiently transfected with a FLAG-FAT10 expression construct and again cycloheximide chase experiments were performed. The FLAG-FAT10 monomer and FLAG-FAT10 conjugates were rapidly degraded and their respective rates of degradation were similar in the IFN-γ stimulated and unstimulated HEK293T cells (Fig. 4). Taken together, we conclude that in both cell line systems tested, FAT10 and FAT10 conjugates were degraded equally fast by the CP and IP.

4. Discussion

The recent discoveries of IP functions that are unrelated to antigen processing have posed the pertinent question as to underlying mechanisms that differ between IP and CP: (1) *Lmp2*$^{-/-}$, *Mecl-1*$^{-/-}$, and *Lmp7*$^{-/-}$ mice are all protected from dextran sodium sulfate (DSS)-induced colitis (Basler et al., 2010; Fitzpatrick et al., 2006; Schmidt et al., 2010). (2) Both *Lmp2*$^{-/-}$ and *Mecl-1*$^{-/-}$ mice show 20–40%

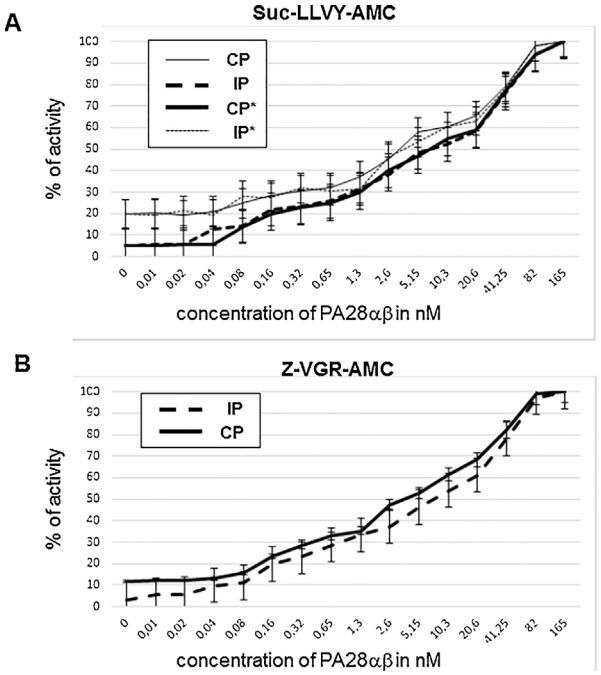

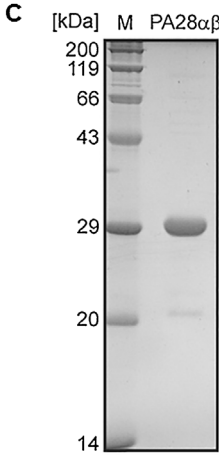

Fig. 1. Equal activation of CP and IP by PA28αβ.
Mouse constitutive proteasome (CP) or immunoproteasome (IP) was incubated with indicated concentrations of mouse recombinant PA28αβ for one hour. Then, digestions of the fluorogenic peptide substrates Suc-LLVY-AMC (A) and Z-VGR-AMC (B) were performed for one hour and the fluorescence of the AMC leaving group was measured. Plotted is the per cent activation by PA28αβ. 20S proteasome preparations labelled with an asterisk had been covalently labelled with a fluorescent dye and were used for thermophoresis experiments shown in Fig. 2. (C) Coomassie-stained SDS-PAGE (15%) of purified recombinant mouse PA28αβ. As PA28α (28.7 kDa) and β (27.1 kDa) subunits show similar in-gel migration behaviour, only one band is observed for PA28αβ.

reductions of $CD8^+$ T cells in lymphoid organs which was shown in mixed bone marrow chimeras to be a T cell intrinsic effect and not due to altered antigen processing (Basler et al., 2006; Van Kaer et al., 1994; Zaiss et al., 2008). (3) The adoptive transfer of IP-deficient but not wild type T cells and B cells into virus-infected mice led to their apoptotic death (Chen et al., 2001; Hensley et al., 2010; Moebius et al., 2010). The need to address a functional difference between IP and CP is further posed by their different expression profiles: while most tissues express mainly CP, lymph nodes, spleen and thymus contain very high levels of IP and this 'constitutively' high IP content at least in the spleen was shown *not* to rely on IFN-γ (Barton et al., 2002). We have shown already in 1997 by Northern blotting that lymphoid tissues not only express much higher mRNA levels for LMP2, MECL-1, and LMP7 but also much lower amounts of β1, β2, and β5 mRNA showing that the strong bias for IP expression in lymphoid tissues is tightly transcriptionally regulated (Stohwasser et al., 1997). Why then do immune cells, among them notoriously poor antigen presenting cells like T cells or NK cells, need high IP rather than CP expression?

One possibility would be that IP degrade or partially process biologically active factors differently than CP. Nevertheless, up to date no evidence for such factors or IP-selective substrates have been identified. Since plain 20S IP and CP exist in the cell in a latent state in which the N-termini of proteasomal α-subunits preclude the entry of folded proteins into the lumen of the 20S particle, the access of protein substrates needs to be facilitated by regulators like the 19S regulator, PA28γ or perhaps PA28αβ which open the entrance of the 20S. Following this rationale, proteasome regulators would need to preferentially bind to either CP or IP in order to enable a differential selection of substrates. The high resolution x-ray crystallographic structures of mouse CP and IP, however, showed identical α-endplates of both proteasome types (Huber et al., 2012) and Stohwasser et al. found that recombinant PA28αβ activated the cleavage of fluorogenic proteasome substrates by CP and IP to the same extent (Stohwasser et al., 2000). Therefore, it came as a surprise when it was recently shown that after protein cross-linking in intact cells, IP-PA28αβ complexes were found in fourfold higher abundance than CP-PA28αβ which did not correlate with the IP/CP distribution in the investigated cells (Fabre et al., 2015). The 19S regulator, in contrast, showed equal binding to the CP and IP while for the proteasome regulator PI31 an eightfold higher association was found with the CP as opposed to the IP. These intriguing findings were an incentive for us to not only compare the effect of PA28αβ on CP and IP activation but also to measure for the first time directly the affinity of

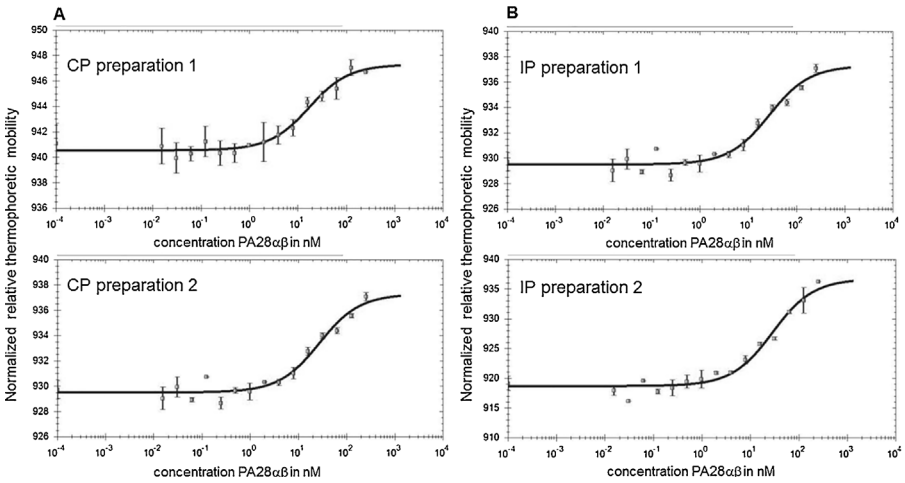

Fig. 2. PA28αβ binds to CP and IP with equal affinity.
Mouse constitutive proteasome (A) or immunoproteasome (B) were labelled with a fluorescent dye. At a concentration of 7.1 nM, proteasomes were incubated for one hour with indicated concentrations of recombinant mouse PA28αβ before determination of the binding affinities in two independent thermopheresis experiments (top and bottom panels) with separate proteasome and PA28αβ preparations. Plotted is the normalized relative thermophoretic mobility of the fluorophore-labelled CP and IP versus the concentration of PA28αβ.

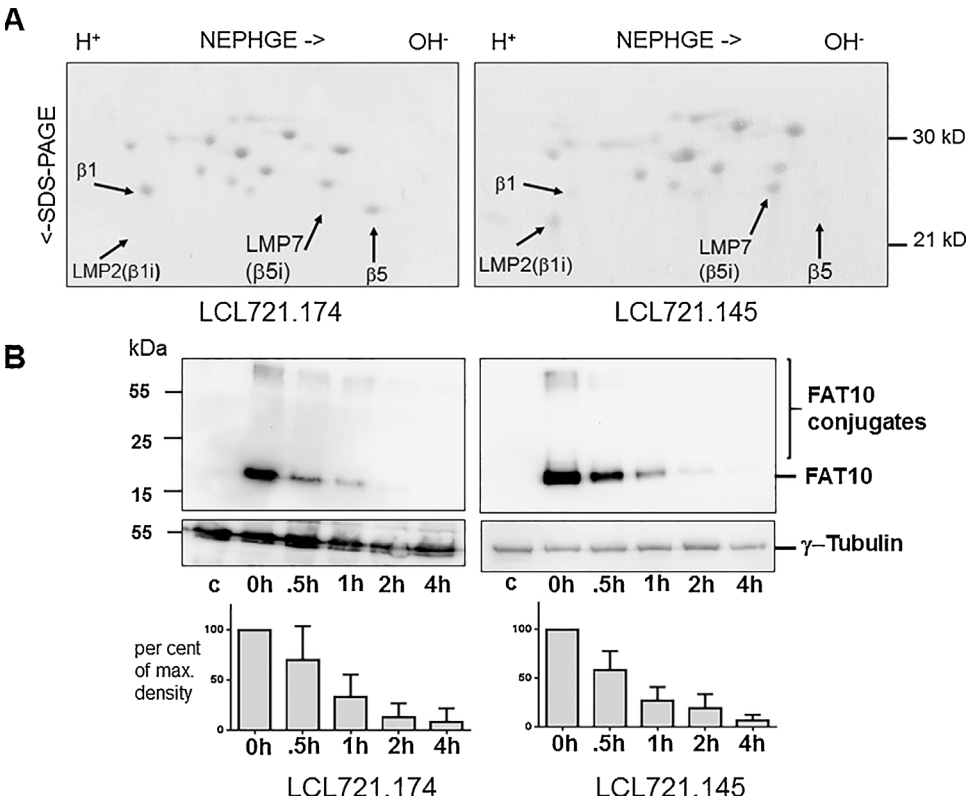

Fig. 3. FAT10 is degraded at the same rate by human B cells expressing CP or IP.
(A) Two-dimensional non equilibrium pH gradient gel electrophoresis (NEPHGE)/SDS-PAGE of purified 20S proteasomes from the CP expressing LMP2/LMP7-deficient B-lymphoblastoid cell line LCL721.174 (left panel) and the B cell line LCL721.145, which expresses high levels of IP. The 20S proteasome subunits were visualized by Coomassie staining. The positions of the subunits β1, LMP2 (β1i), β5, and LMP7 (β5i) are indicated by arrows. (B) The cell lines LCL721.174 (left panels) and LCL721.145 (right panels) were transduced with a lentivirus encoding 3xFLAG-hFAT10 and GFP, and after three days cycloheximide chase experiments were performed for the indicated time periods followed by western blotting for FLAG-FAT10 and γ-tubulin loading control as indicated. The graphs below the blots show the means +/− SEM of three independent experiments with similar outcomes.

PA28αβ-binding to the CP and IP.

The thermophoresis method, which we have used, bears the potential caveat that one of the binding partners has to carry a fluorophore. We labelled the purified CP and IP by N-Hydroxysuccinimide (NHS) technology via the primary amine of lysines in the proteasome and used a molar dye to proteasome ratio of 5:1. This means that a maximum of five lysines per proteasome will be randomly labelled which is probably negligible for regulator-binding to a 700 kDa complex and which is very unlikely to result in a bias for or against CP vs. IP. Nevertheless, to exclude a disturbing effect of the bound dye on the binding and functional properties of mouse CP and IP, we compared the activation of the labelled and unlabelled proteasomes by titrated amounts of PA28αβ side by side using the fluorogenic substrates Suc-LLVY-AMC (chymotrypsin-like activity) and Z-VGR-AMC (trypsin-like activity) (Fig. 1). We found no significant difference between the labelled and unlabelled 20S proteasomes thus demonstrating that the thermophoresis approach is valid to measure the affinities of CP and IP for PA28αβ. We found in the activation assays that CP and IP were equally activated by PA28αβ in agreement with a previous report (Stohwasser et al., 2000). In two independent thermophoresis experiments we obtained the affinity constants of 12.2 nM +/− 2.8 nM for PA28αβ-binding to mouse CP (Fig. 2A) and 15.3 nM +/− 2.7 nM for PA28αβ-binding to mouse IP (Fig. 2B). These values differ considerably from the affinity constants deduced from the previously reported activation assays, which were 100 nM for PA28αβ-binding to CP and 88 nM for PA28 αβ-binding to IP (Stohwasser et al., 2000). Notably, Stohwasser et al. reconstituted the PA28αβ heterocomplex from individually purified recombinant mouse PA28 α and β subunits, whereas the PA28αβ preparation for our study was obtained by co-expression of both subunits in *E. coli*. Thus, our PA28αβ samples and those used by Stohwasser et al. might differ in the stoichiometry of α and β entities. Moreover, these authors used 20S proteasomes purified from the mouse fibroblast line B8 which expresses considerable amounts of LMP7 (but not LMP2) as source of 'CP', and the LMP2/MECL-1/LMP7 triple transfectant of B8 as a source of IP (Groettrup et al., 1997). In contrast, we used 20S proteasomes purified from the livers of *Lmp7*$^{-/-}$*Mecl-1*$^{-/}$

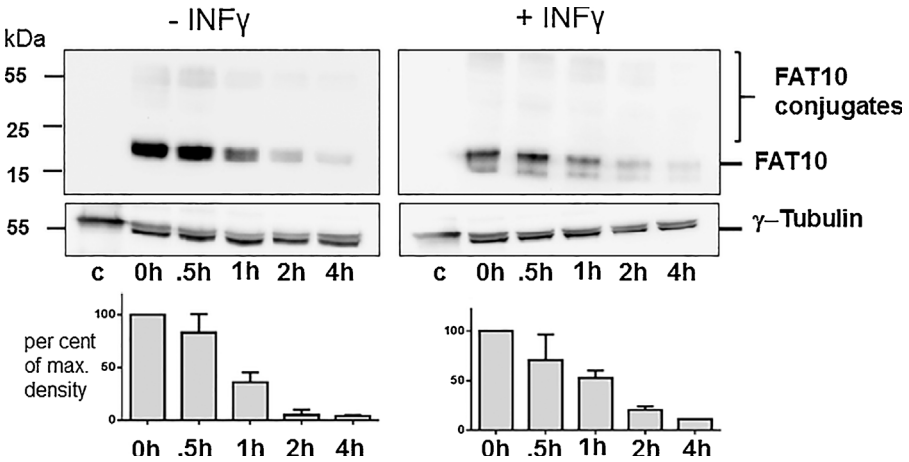

Fig. 4. FAT10 is degraded equally fast in HEK293T cells before and after IFN-γ stimulation.
The human embryonic kidney cell line HEK293T was stimulated or not with IFN-γ for two days and then transiently transfected with a 3xFLAG-hFAT10 expression construct. After one further day of IFN-γ stimulation, cycloheximide chase experiments were performed for the indicated time periods followed by western blotting for FLAG-FAT10 and γ-tubulin loading control as indicated. The graphs below the blots show the means +/− SEM of three independent experiments with similar outcomes.

− mice and LCMV-infected wild type mice. Another source of discrepany could be that the kinetic models used to calculate the affinity constants by Stohwasser et al. did not adequately mirror the binding of the 20S proteasomes to PA28αβ. Remarkably, in another publication, the same group published an affinity constant for B8-derived immunoproteasome and PA28αβ purified from cells ectopically expressing mouse PA28αβ of 44.4 μM (van Hall et al., 2000) which is quite different from our results and those reported by Stohwasser et al. Nevertheless, both the latter studies and our data agree that PA28αβ activates and binds to CP and IP equally. How can this result be reconciled with a preferential association of PA28αβ and IP within cells as reported by Fabre et al. (Fabre et al., 2015)? One possibility is that the interaction surfaces of the 20S IP or CP or PA28αβ get post-translationally modified in cells which would not be represented by recombinant PA28αβ. In this respect it is interesting to note that there is increasing and convincing evidence that the activity of the 26S proteasome is regulated by phosphorylation (Guo et al., 2016; Lokireddy et al., 2015). Since the preparations of mouse CP and IP, which we have used in this study, and previously for determination of the three-dimensional structures of the CP and IP (Huber et al., 2012), have been purified in the absence of phosphatase inhibition, we cannot rule out that in cells the IP and CP may be differentially phosphorylated which might affect their association with proteasome regulators.

Both types of curves, obtained with thermophoresis or by the analysis of peptide cleavage activation, do not provide any evidence that two binding sites may exist. Because it is known how PA28 binds to the proteasome (Gray et al., 1994; Knowlton et al., 1997; Whitby et al., 2000; Sprangers and Kay, 2007; Huber et al., 2012), the conclusion can be drawn that both α-endplates of the proteasome are bound by PA28αβ with the same affinity. That means that the calculated affinity is correct for the 20S proteasome, but because each proteasome has two α-endplates, the affinity for each plate is two times lower. Another important conclusion can be drawn from the comparison of the binding curves. The maximal stimulation of peptide cleavage is achieved at maximum binding of PA28. That means the proteasome can take up substrates at the same time from both sites and possibly use both β-rings for catalytic processing.

The second IFN-γ/TNF induced factor, which we investigated for a preferential cooperation with CP or IP, was the ubiquitin-like modifier FAT10. The rapid, well reproducible and entirely proteasome-dependent degradation of FAT10 (Aichem et al., 2014; Rani et al., 2012; Spinnenhirn et al., 2014) served as a read out in two different cell lines. In the CP-containing LCL721.174 and IP-containing LCL721.145 cells FLAG-FAT10 was degraded at the same rate (Fig. 3). These two clones, both derived from the human B cell line LCL721, were ideal for this investigation because they expressed almost exclusively CP and IP, respectively. In order to study FAT10 degradation in a cell line which expresses no detectable IP in the absence of stimulation and very high levels of IP after three days of stimulation with IFN-γ and TNF (Fabre et al., 2015), we performed a second series of experiments in HEK293T cells. Again ectopically expressed FLAG-FAT10 was degraded at the same rate in the absence and presence of cytokine-induced IP expression. Thus, also in the physiological situation of IFN-γ stimulation, the degradation rate of FAT10 by CP and IP was the same. A slight disadvantage of this system may be that in IFN-γ-stimulated cells low levels of endogenous FAT10 are expressed in addition to the monitored ectopically expressed FLAG-FAT10 (Raasi et al., 1999). However, in contrast to the IP, which is fully induced by sole stimulation with IFN-γ, strong FAT10 induction occurs only when HEK293T cells are stimulated both, with IFN-γ and TNF (Aichem et al., 2010; Raasi et al., 1999). Apparently, the low level of endogenous FAT10 induced by IFN-γ alone in HEK293T cells did not affect the degradation rate of ectopic FLAG-FAT10 (Fig. 4), suggesting that the proteasomal degradation capacity for FAT10 and its conjugates was not limiting. Since FAT10 binds to the 26S proteasome via the 19S regulator subunit RPN10 (Rani et al., 2012), our results suggest that the 20S CP and IP associate equally well with the 19S regulator which is in accordance with cross-linking (Fabre et al., 2015) and structural studies (Huber et al., 2012).

In conclusion, we show in this study that PA28αβ equally activates and binds to CP and IP and that FAT10 is degraded by both proteasome types at the same rate. Therefore it will be pertinent to search for further molecular and mechanistic differences between CP and IP which may account for their unique functions in cytokine production, T helper cell differentiation, lymphocyte survival as well as the pathogenesis of autoimmune diseases, colon cancer, and transplant rejection.

Conflict of interests

The authors declare no conflicts of interest.

Funding

This work was supported by grants BA4199/2-1 and GR1517/14-1 from the German Research Foundation (DFG) and the DFG Collaborative Research Center SFB969, project C01 (to M. G.). E. M. H. acknowledges financial support by the Peter und Traudl Engelhorn-Stiftung and the Young Scholars Programme of the Bavarian Academy of Sciences and Humanities. R.S. is a member of the Konstanz Research School Chemical Biology funded by the German Excellence Initiative. The funders had no role in the study design, nor in the collection, analysis, and interpretation of the data, writing of the report, and decision to submit the article for publication.

Acknowledgements

We thank C. Wünsch for excellent technical assistance, Christian Schmidt for help with preparing the graphical abstract, and the personnel of the Animal Research Facility of Konstanz University for dedicated animal care taking.

References

Ahn, K., Erlander, M., Leturcq, D., Peterson, P.A., Früh, K., Yang, Y., 1996. In Vivo characterization of the proteasome regulator PA28. J. Biol. Chem. 271, 18237–18242.

Aichem, A., Pelzer, C., Lukasiak, S., Kalveram, B., Sheppard, P.W., Rani, N., Schmidtke, G., Groettrup, M., 2010. USE1 is a bispecific conjugating enzyme for ubiquitin and FAT10, which FAT10ylates itself in cis. Nat. Commun. 1, 13.

Aichem, A., Kalveram, B., Spinnenhirn, V., Kluge, K., Catone, N., Johansen, T., Groettrup, M., 2012. The proteomic analysis of endogenous FAT10 substrates identifies p62/SQSTM1 as a substrate of FAT10ylation. J. Cell Sci. 125, 4576–4585.

Aichem, A., Catone, N., Groettrup, M., 2014. Investigations into the auto-FAT10ylation of the bispecific E2 conjugating enzyme UBA6-specific E2 enzyme 1. FEBS J. 281, 1848–1859.

Barton, L.F., Cruz, M., Rangwala, R., Deepe, G.S., Monaco, J.J., 2002. Regulation of immunoproteasome subunit expression in vivo following pathogenic fungal infection. J. Immunol. 169, 3046–3052.

Basler, M., Moebius, J., Elenich, L., Groettrup, M., Monaco, J.J., 2006. An altered T cell repertoire in MECL-1-deficient mice. J. Immunol. 176, 6665–6672.

Basler, M., Dajee, M., Moll, C., Groettrup, M., Kirk, C.J., 2010. Prevention of experimental colitis by a selective inhibitor of the immunoproteasome. J. Immunol. 185, 634–641.

Basler, M., Mundt, S., Muchamuel, T., Moll, C., Jiang, J., Groettrup, M., Kirk, C.J., 2014. Inhibition of the immunoproteasome ameliorates experimental autoimmune encephalomyelitis. EMBO Mol. Med. 6, 226–238.

Bates, E.F.M., Ravel, O., Dieu, M.C., Ho, S., Guret, C., Bridon, J.M., AitYahia, S., Briere, F., Caux, C., Banchereau, J., Lebecque, S., 1997. Identification and analysis of a novel member of the ubiquitin family expressed in dendritic cells and mature B cells. Eur. J. Immunol. 27, 2471–2477.

Boes, B., Hengel, H., Ruppert, T., Multhaup, G., Koszinowski, U.H., Kloetzel, P.M., 1994. Interferon γ stimulation modulates the proteolytic activity and cleavage site preference of 20S mouse proteasomes. J. Exp. Med. 179, 901–909.

Buerger, S., Herrmann, V.L., Mundt, S., Trautwein, N., Groettrup, M., Basler, M., 2015. The ubiquitin-like modifier FAT10 is selectively expressed in medullary thymic epithelial cells and modifies t cell selection. J. Immunol. 195, 4106–4116.

Cascio, P., Call, M., Petre, B.M., Walz, T., Goldberg, A.L., 2002. Properties of the hybrid form of the 26S proteasome containing both 19S and PA28 complexes. EMBO J. 21, 2636–2645.

Chen, W.S., Norbury, C.C., Cho, Y.J., Yewdell, J.W., Bennink, J.R., 2001. Immunoproteasomes shape immunodominance hierarchies of antiviral CD8(+) T cells at the levels of T cell repertoire and presentation of viral antigens. J. Exp. Med. 193, 1319–1326.

Chiu, Y., Sun, Q., Chen, Z., 2007. E1-L2 activates both ubiquitin and FAT10. Mol. Cell 27, 1014–1023.
Collins, G.A., Goldberg, A.L., 2017. The logic of the 26S proteasome. Cell 169, 792–806.
De, M., Jayarapu, K., Elenich, L., Monaco, J.J., Colbert, R.A., Griffin, T.A., 2003. Beta 2 subunit propeptides influence cooperative proteasome assembly. J. Biol. Chem. 278, 6153–6159.
de Graaf, N., van Helden, M.J.G., TextorisTaube, K., Chiba, T., Topham, D.J., Kloetzel, P.M., Zaiss, D.M.W., Sijts, A.J.A.M., 2011. PA28 and the proteasome immunosubunits play a central and independent role in the production of MHC class I-binding peptides in vivo. Eur. J. Immunol. 41, 926–935.
Dick, T.P., Ruppert, T., Groettrup, M., Kloetzel, P.M., Kuehn, L., Koszinowski, U.H., Stevanović, S., Schild, H., Rammensee, H.-G., 1996. Coordinated dual cleavages by the proteasome regulator PA28 lead to dominant MHC ligands. Cell 86, 253–262.
Driscoll, J., Brown, M.G., Finley, D., Monaco, J.J., 1993. MHC-linked LMP gene products specifically alter peptidase activities of the proteasome. Nature 365, 262–264.
Dubiel, W., Pratt, G., Ferrell, K., Rechsteiner, M., 1992. Purification of an 11S regulator of the multicatalytic proteinase. J. Biol. Chem. 267, 22369–22377.
Ebstein, F., Lehmann, A., Kloetzel, P.M., 2012. The FAT10- and ubiquitin-dependent degradation machineries exhibit common and distinct requirements for MHC class I antigen presentation. Cell. Mol. Life Sci. 69, 2443–2454.
Fabre, B., Lambour, T., Garrigues, L., Amalric, F., Vigneron, N., Menneteau, T., Stella, A., Monsarrat, B., Van den Eynde, B., Burlet-Schiltz, O., Bousquet-Dubouch, M.P., 2015. Deciphering preferential interactions within supramolecular protein complexes: the proteasome case. Mol. Syst. Biol. 11, 771.
Fehling, H.J., Swat, W., Laplace, C., Kuehn, R., Rajewsky, K., Mueller, U., von Boehmer, H., 1994. MHC class I expression in mice lacking proteasome subunit LMP-7. Science 265, 1234–1237.
Fitzpatrick, L.R., Khare, V., Small, J.S., Koltun, W.A., 2006. Dextran sulfate sodium-induced colitis is associated with enhanced low molecular mass polypeptide 2 (LMP2) expression and is attenuated in LMP2 knockout mice. Digest Dis. Sci. 51, 1269–1276.
Gaczynska, M., Rock, K.L., Goldberg, A.L., 1993. Gamma-interferon and expression of MHC genes regulate peptide hydrolysis by proteasomes. Nature 365, 264–267.
Gray, C.W., Slaughter, C.A., DeMartino, G.N., 1994. PA28 activator protein forms regulatory caps on proteasome stacked rings. J. Mol. Biol. 236, 7–15.
Groettrup, M., Ruppert, T., Kuehn, L., Seeger, M., Standera, S., Koszinowski, U., Kloetzel, P.M., 1995. The interferon-γ-inducible 11S regulator (PA28) and the LMP2/LMP7 subunits govern the peptide production by the 20S proteasome in vitro. J. Biol. Chem. 270, 23808–23815.
Groettrup, M., Kraft, R., Kostka, S., Standera, S., Stohwasser, R., Kloetzel, P.-M., 1996a. A third interferon-γ-induced subunit exchange in the 20S proteasome. Eur. J. Immunol. 26, 863–869.
Groettrup, M., Soza, A., Eggers, M., Kuehn, L., Dick, T.P., Schild, H., Rammensee, H.-G., Koszinowski, U.H., Kloetzel, P.-M., 1996b. A role for the proteasome regulator PA28α in antigen presentation. Nature 381, 166–168.
Groettrup, M., Standera, S., Stohwasser, R., Kloetzel, P.M., 1997. The subunits MECL-1 and LMP2 are mutually required for incorporation into the 20S proteasome. Proc. Natl. Acad. Sci. U. S. A. 94, 8970–8975.
Groettrup, M., Pelzer, C., Schmidtke, G., Hofmann, K., 2008. Activating the ubiquitin family: UBA6 challenges the field. Tr. Biochem. Sci. 33, 230–237.
Groettrup, M., Kirk, C.J., Basler, M., 2010. Proteasomes in immune cells: more than peptide producers? Nat. Rev. Immunol. 10, 72–77.
Guo, X., Wang, X., Wang, Z., Banerjee, S., Yang, J., Huang, L., Dixon, J.E., 2016. Site-specific proteasome phosphorylation controls cell proliferation and tumorigenesis. Nat. Cell Biol. 18, 202–212.
Hensley, S.E., Zanker, D., Dolan, B.P., David, A., Hickman, H.D., Embry, A.C., Skon, C.N., Grebe, K.M., Griffin, T.A., Chen, W.S., Bennink, J.R., Yewdell, J.W., 2010. Unexpected role for the immunoproteasome subunit LMP2 in antiviral humoral and innate immune responses. J. Immunol. 184, 4115–4122.
Hipp, M.S., Kalveram, B., Raasi, S., Groettrup, M., Schmidtke, G., 2005. FAT10, a ubiquitin-independent signal for proteasomal degradation. Mol. Cell Biol. 25, 3483–3491.
Huber, E.M., Groll, M., 2017. The mammalian proteasome activator PA28 forms an asymmetric α4β3 complex. Structure 25, 1473–1480.
Huber, E.M., Basler, M., Schwab, R., Heinemeyer, W., Kirk, C.J., Groettrup, M., Groll, M., 2012. Immuno- and constitutive proteasome crystal structures reveal differences in substrate and inhibitor specificity. Cell 148, 727–738.
Ichikawa, H.T., Conley, T., Muchamuel, T., Jiang, J., Lee, S., Owen, T., Barnard, J., Nevarez, S., Goldman, B.I., Kirk, C.J., Looney, R.J., Anolik, J.H., 2012. Beneficial effect of novel proteasome inhibitors in murine lupus via dual inhibition of type I interferon and autoantibody-secreting cells. Arthritis Rheum. 64, 493–503.
Kalim, K.W., Basler, M., Kirk, C.J., Groettrup, M., 2012. Immunoproteasome subunit LMP7 deficiency and inhibition suppresses Th1 and Th17 but enhances regulatory T cell differentiation. J. Immunol. 189, 4182–4193.
Kavathas, P., Bach, F.H., DeMars, R., 1980. Gamma ray-induced loss of expression of HLA and glyoxalase I alleles in lymphoblastoid cells. Proc. Natl. Acad. Sci. U. S. A. 77, 4251–4255.
Khan, S., van den Broek, M., Schwarz, K., de Giuli, R., Diener, P.A., Groettrup, M., 2001. Immunoproteasomes largely replace constitutive proteasomes during an antiviral and antibacterial immune response in the liver. J. Immunol. 167, 6859–6868.
Knowlton, J.R., Johnston, S.C., Whitby, F.G., Realini, C., Zhang, Z.G., Rechsteiner, M., Hill, C.P., 1997. Structure of the proteasome activator REG alpha (PA28 alpha). Nature 390, 639–643.
Koerner, J., Brunner, T., Groettrup, M., 2017. Inhibition and deficiency of the immunoproteasome subunit LMP7 suppress the development and progression of colorectal carcinoma in mice. Oncotarget 8, 50873–50888.
Kremer, M., Henn, A., Kolb, C., Basler, M., Moebius, J., Guillaume, B., Leist, M., VandenEynde, B.J., Groettrup, M., 2010. Reduced immunoproteasome formation and accumulation of immunoproteasomal precursors in the brains of lymphocytic choriomeningitis virus-Infected mice. J. Immunol. 185, 5549–5560.
Kuehn, L., Dahlmann, B., 1996. Reconstitution of proteasome activator PA 28 from isolated subunits: optimal activity is associated with an α,β-heteromultimer. FEBS Lett. 394, 183–186.
Li, X.T., Lonard, D.M., Jung, S.Y., Malovannaya, A., Feng, G., Qin, J., Tsai, S.Y., Tsai, M.J., OMalley, B.W., 2006. The SRC-3/AIB1 coactivator is degraded in a ubiquitin- and ATP- independent manner by the REG gamma proteasome. Cell 124, 381–392.
Liu, Y., Pan, J., Zhang, C., Fan, W., Collinge, M., Bender, J.R., Weissman, S.M., 1999. A MHC-encoded ubiquitin-like protein (FAT10) binds noncovalently to the spindle assembly checkpoint protein MAD2. Proc. Natl. Acad. Sci. U. S. A. 96, 4313–4318.
Lokireddy, S., Kukushkin, N.V., Goldberg, A.L., 2015. cAMP-induced phosphorylation of 26S proteasomes on Rpn6/PSMD11 enhances their activity and the degradation of misfolded proteins. Proc. Natl. Acad. Sci. U. S. A. 112, E7176–85.
Lukasiak, S., Schiller, C., Oehlschlaeger, P., Schmidtke, G., Krause, P., Legler, D.F., Autschbach, F., Schirmacher, P., Breuhahn, K., Groettrup, M., 2008. Proinflammatory cytokines cause FAT10 upregulation in cancers of liver and colon. Oncogene 27, 6068–6074.
Ma, C.-P., Slaughter, C.A., DeMartino, G.N., 1992. Identification, purification and characterization of a protein activator (PA28) of the 20S Proteasome (Macropain). J. Biol. Chem. 267, 10515–10523.
Moebius, J., vandenBroek, M., Groettrup, M., Basler, M., 2010. Immunoproteasomes are essential for survival and expansion of T cells in virus-infected mice. Eur. J. Immunol. 40, 3439–3449.
Moriishi, K., Okabayashi, T., Nakai, K., Moriya, K., Koike, K., Murata, S., Chiba, T., Tanaka, K., Suzuki, R., Suzuki, T., Miyamura, T., Matsuura, Y., 2003. Proteasome activator PA28 gamma-dependent nuclear retention and degradation of hepatitis C virus core protein. J. Virol. 77, 10237–10249.
Muchamuel, T., Basler, M., Aujay, M.A., Suzuki, E., Kalim, K.W., Lauer, C., Sylvain, C., Ring, E.R., Shields, J., Jiang, J., Shwonek, P., Parlati, F., Demo, S.D., Bennett, M.K., Kirk, C.J., Groettrup, M., 2009. A selective inhibitor of the immunoproteasome subunit LMP7 blocks cytokine production and attenuates progression of experimental arthritis. Nat. Med. 15, 781–787.
Murata, S., Udono, H., Tanahashi, N., Hamada, N., Watanabe, K., Adachi, K., Yamano, T., Yui, K., Kobayashi, N., Kasahara, M., Tanaka, K., Chiba, T., 2001. Immunoproteasome assembly and antigen presentation in mice lacking both PA28 alpha and PA28 beta. EMBO J. 20, 5898–5907.
Nagayama, Y., Nakahara, M., Shimamura, M., Horie, I., Arima, K., Abiru, N., 2012. Prophylactic and therapeutic efficacies of a selective inhibitor of the immunoproteasome for Hashimoto's thyroiditis but not for Graves' hyperthyroidism, in mice. Clin. Exp. Immunol. 168, 268–273.
Raasi, S., Schmidtke, G., de Giuli, R., Groettrup, M., 1999. A ubiquitin-like protein which is synergistically inducible by interferon-γ and tumor necrosis factor-α. Eur. J. Immunol. 29, 4030–4036.
Rani, N., Aichem, A., Schmidtke, G., Kreft, S.G., Groettrup, M., 2012. FAT10 and NUB1L bind to the VWA domain of Rpn10 and Rpn1 to enable proteasome-mediated proteolysis. Nat. Commun. 3, 749.
Realini, C., Jensen, C.C., Zhang, Z.G., Johnston, S.C., Knowlton, J.R., Hill, C.P., Rechsteiner, M., 1997. Characterization of recombinant REG alpha, REG beta, and REG gamma proteasome activators. J. Biol. Chem. 272, 25483–25492.
Schliehe, C., Bitzer, A., van den Broek, M., Groettrup, M., 2012. Stable antigen is most effective for eliciting CD8+ T-cell responses after DNA vaccination and infection with recombinant vaccinia virus in vivo. J. Virol. 86, 9782–9793.
Schmidt, N., Gonzalez, E., Visekruna, A., Kuhl, A.A., Loddenkemper, C., Mollenkopf, H., Kaufmann, S.H.E., Steinhoff, U., Joeris, T., 2010. Targeting the proteasome: partial inhibition of the proteasome by bortezomib or deletion of the immunosubunit LMP7 attenuates experimental colitis. Gut 59, 896–906.
Schmidtke, G., Emch, S., Groettrup, M., Holzhütter, H.G., 2000. Evidence for the existence of a non-catalytic modifier site of peptide hydrolysis by the 20S proteasome. J. Biol. Chem. 275, 22056–22063.
Schmidtke, G., Kalveram, B., Groettrup, M., 2009. Degradation of FAT10 by the 26S proteasome is independent of ubiquitylation but relies on NUB1L. FEBS Lett. 583, 591–594.
Schwarz, K., Eggers, M., Soza, A., Koszinowski, U.H., Kloetzel, P.M., Groettrup, M., 2000. The proteasome regulator PA28α/β can enhance antigen presentation without affecting 20S proteasome subunit composition. Eur. J. Immunol. 30, 3672–3679.
Schweitzer, A., Aufderheide, A., Rudack, T., Beck, F., Pfeifer, G., Plitzko, J.M., Sakata, E., Schulten, K., Foerster, F., Baumeister, W., 2016. Structure of the human 26S proteasome at a resolution of 3.9 angstrom. Proc. Natl. Acad. Sci. U. S. A. 113, 7816–7821.
Song, X., Mott, J.D., Kampen J. v. Pramanik, B., Tanaka, K., Slaughter, C.A., DeMartino, G.N., 1996. A model for the quarternary structure of the proteasome activator PA 28. J. Biol. Chem. 271, 26410–26417.
Spinnenhirn, V., Farhan, H., Basler, M., Aichem, A., Canaan, A., Groettrup, M., 2014. The ubiquitin-like modifier FAT10 decorates autophagy-targeted Salmonella and contributes to Salmonella resistance in mice. J. Cell Sci. 127, 4883–4893.
Sprangers, R., Kay, L.E., 2007. Quantitative dynamics and binding studies of the 20S proteasome by NMR. Nature 445, 618–622.
Stohwasser, R., Standera, S., Peters, I., Kloetzel, P.-M., Groettrup, M., 1997. Molecular cloning of the mouse proteasome subunits MC14 and MECL-1: reciprocally regulated tissue expression of interferon-γ − modulated proteasome subunits. Eur. J. Immunol. 27, 1182–1187.
Stohwasser, R., Salzmann, U., Giesebrecht, J., Kloetzel, P.M., Holzhütter, H.G., 2000. Kinetic evidences for facilitation of peptide channelling by the proteasome activator PA28. Eur. J. Biochem. 267, 6221–6230.

Tenzer, S., Stoltze, L., Schonfisch, B., Dengjel, J., Muller, M., Stevanovic, S., Rammensee, H.G., Schild, H., 2004. Quantitative analysis of prion-protein degradation by constitutive and immuno-20S proteasomes indicates differences correlated with disease susceptibility. J. Immunol. 172, 1083–1091.

Theng, S.S., Wang, W., Mah, W.-C., Chan, C., Zhuo, J., Gao, Y., Qin, H., Lim, L., Chong, S.S., Song, J., Lee, C.G., 2014. Disruption of FAT10-MAD2 binding inhibits tumor progression. Proc. Natl. Acad. Sci. U. S. A. 111, E5282–E5291.

Toes, R.E.M., Nussbaum, A.K., Degermann, S., Schirle, M., Emmerich, N.P.N., Kraft, M., Laplace, C., Zwinderman, A., Dick, T.P., Muller, J., Schonfisch, B., Schmid, C., Fehling, H.J., Stevanovic, S., Rammensee, H.G., Schild, H., 2001. Discrete cleavage motifs of constitutive and immunoproteasomes revealed by quantitative analysis of cleavage products. J. Exp. Med. 194, 1–12.

Vachharajani, N., Joeris, T., Luu, M., Hartmann, S., Pautz, S., Jenike, E., Pantazis, G., Prinz, I., Hofer, M.J., Steinhoff, U., Visekruna, A., 2017. Prevention of colitis-associated cancer by selective targeting of immunoproteasome subunit LMP7. Oncotarget 8, 50447–50459.

van Hall, T., Sijts, A., Camps, M., Offringa, R., Melief, C., Kloetzel, P.M., Ossendorp, F., 2000. Differential influence on cytotoxic T lymphocyte epitope presentation by controlled expression of either proteasome immunosubunits or PA28. J. Exp. Med. 192, 483–494.

Van Kaer, L., Ashton-Rickardt, P.G., Eichelberger, M., Gaczynska, M., Nagashima, K., Rock, K.L., Goldberg, A.L., Doherty, P.C., Tonegawa, S., 1994. Altered peptidase and viral-specific T cell response in LMP 2 mutant mice. Immunity 1, 533–541.

Whitby, F.G., Masters, E.I., Kramer, L., Knowlton, J.R., Yao, Y., Wang, C.C., Hill, C.P., 2000. Structural basis for the activation of 20S proteasomes by 11S regulators. Nature 408, 115–120.

Yamano, T., Murata, S., Shimbara, N., Tanaka, N., Chiba, T., Tanaka, K., Yui, K., Udono, H., 2002. Two distinct pathways mediated by PA28 and hsp90 in major histocompatibility complex class I antigen processing. J. Exp. Med. 196, 185–196.

Zaiss, D.M., de Graaf, N., Sijts, A.J., 2008. The proteasome immunosubunit multicatalytic endopeptidase complex-like 1 is a T-cell-intrinsic factor influencing homeostatic expansion. Infect. Immun. 76, 1207–1213.

Zhang, Z., Zhang, R.W., 2008. Proteasome activator PA28gamma regulates p53 by enhancing its MDM2- mediated degradation. EMBO J. 27, 852–864.

Zhang, Z.G., Krutchinsky, A., Endicott, S., Realini, C., Rechsteiner, M., Standing, K.G., 1999. Proteasome activator 11S REG or PA28: recombinant REG alpha/REG beta hetero-oligomers are heptamers. Biochemistry 38, 5651–5658.